Article

Reducing Peak Power in a Multiple Load System by Delaying the Activation of Electrical Loads Using a Filter Based on a PI Controller

Jerzy Kasprzyk [1,*] and Michał Szulc [1,2]

1   Department of Measurements and Control Systems, Silesian University of Technology, Akademicka 16, 44-100 Gliwice, Poland; michal.szulc@git.lukasiewicz.gov.pl
2   Łukasiewicz Research Network—Upper Silesian Institute of Technology, Miarki 12-14, 44-100 Gliwice, Poland
*   Correspondence: jerzy.kasprzyk@polsl.pl

Abstract: In a power grid with multiple two-state loads, the total power can vary over a significant range. This results in the inability to supply this system from a low-power source. The solution is an algorithm that shapes energy demand depending on its availability. For this purpose, a new load distribution method is proposed based on introducing a buffer between the temperature controller output and the heater and filtering the load using a master Proportional–Integral (PI) controller. The aim of the work was to evaluate the quality of the developed algorithm for limiting power peaks in the power grid. The research was conducted on a model of the Creep Test Laboratory with 389 heaters simulated in MATLAB Simulink R2023b. The algorithm was tested with various settings of the master controller parameters. By experimentally adjusting these parameters, a ten-fold reduction in peak power was achieved. The standard deviation for the L1 phase was reduced from 7.6 kW to 0.6 kW. Similar results were obtained for phases L2 and L3. The tested control system tracked changes in the average power value by changing the number of loads switched on and by frequency-modulating the signal when the change was less than the power of a single load. It was demonstrated that the controlled delayed switching of electrical loads can modify the shape of the total electric power without affecting their operation. The proposed solution features a low computational complexity, which allows its implementation in various systems.

Keywords: load shifting; power shortage; virtual energy storage (VES); scheduling; electric heating load; creep test; off-grids; PI controller

1. Introduction

The energy transition and the related increase in the share of renewables in the energy mix are leading to increasing discussions about abandoning the current energy model, in which the electricity source has sufficient power to cover the needs of all consumers. This model assumed that the power grid would always have the capacity to meet the needs of all customers at any given time. This was easy to implement because energy was supplied to the grid only stable and predictable sources processing fossil fuels. The increase in the share of renewable power on the grid has resulted in either a surplus or a shortage of energy at constant load. A deficit of generated electricity causes temporary shortages in some areas. However, a surplus of energy has the effect of raising the voltage in the electricity grid, which can cause damage to electrical appliances. Temporary deficits in the availability of energy are now compensated via cross-border exchanges. Similarly, this occurs in the case of surpluses [1,2]. However, increasing the share of renewable sources in the energy grid also in neighbouring countries generates the risk that these countries will not be able to receive the surplus energy [3,4]. With a large percentage of energy coming from photovoltaics and wind farms, where these sources are highly dependent on weather conditions, this situation can occur quite often. This results in the need to switch off part of the energy

sources connected to the grid. Renewable energy sources are the most frequently shut down [5–7]. This is due to the impossibility of rapidly shutting down large fossil fuel-based power units. It is important to note that frequent shutdowns of large power units involve a significant reduction in their operating time [8,9]. Fluctuations in the output of renewable sources driven by changes in the weather destabilise the electricity grid. A solution to this is the use of local energy storage units to receive surplus energy and compensate for deficits. This is a proven solution but requires a relatively significant investment for their implementation [10–13]. Another way to handle the problems related to changing energy availability is to reverse the role of supplier-consumer. With this solution, the energy supplier does not guarantee immediate availability but, depending on the situation distributes the energy in such a way as to make optimal use of the available power at a given time [14–17]. In this model, the energy consumer makes a request for power, while the electricity grid manager decides when it will be supplied. The simplest form of this type of communication between power source and receiver is implemented in the USB-C link protocol, where the receiver communicates with the source to agree on how much power it expects and how much power can be delivered to it from the power source [18,19]. With the rapidly evolving infrastructure of the Internet of Things, a standard can be established at which each device that is plugged into the network negotiates its needs and limitations with the network manager. The way in which the master controller shapes the total power supply will depend on the type and availability of the power sources connected to the network [20–22]. A comprehensive review of control and estimation techniques used in smart microgrids, such as linear, non-linear, robust, predictive, intelligent and adaptive, can be found in [23].

In this paper, the problem of reducing power peaks occurring in a microgrid with many loads is considered. A new load distribution method is proposed based on introducing a buffer between the temperature controller output and the heater and filtering the load using a master PI controller. The quality of the developed algorithm was tested on a model of the Creep Test Laboratory with 389 heaters simulated in MATLAB Simulink R2023b.

2. Materials and Methods

The work focuses on solving a practical problem that occurs in a large Creep Test Laboratory, which is a part of the Łukasiewicz Research Network—Upper Silesian Institute of Technology in Gliwice, Poland.

2.1. Creep Test Laboratory

The laboratory consists of 89 single-sample creep test machines and four two-chamber multi-sample creep test machines. As a result, nearly 900 samples can be tested simultaneously in the laboratory [24]. The single-sample creep test machines are shown in Figure 1a, and the multi-sample creep test machines are shown in Figure 1b.

Figure 1. (**a**) One-sample creep test machines, (**b**) multi-sample creep test machines.

The laboratory focuses mainly on the research of steel and metal alloys. The results of the research are applied in the energy [25], petrochemical [26], and aerospace industries, as well as in other industries where the material used is exposed to high stress and high temperature [27]. Creep tests are conducted over a long period of time. The duration of a single test can range from tens of hours to even decades. The test preparation and conduct process is described in the standard Metallic materials—Uniaxial creep testing in tension—Method of test (ISO 204:2023) [28]. In order to meet the requirements of the standard, the laboratory has been completely automated. One of the requirements is to conduct creep testing continuously. Due to this fact, the laboratory has been equipped with a diesel generator to ensure the availability of electricity in the event of its loss in the mains. The power of the generator was specified with some margin to match the power of the laboratory, where all the creep test machines are running, and the air conditioning system is in operation. The typical average load generated by the laboratory does not exceed 60 kW, while the rated power of the generator is 75 kW. This shows that the generator has been selected with a reserve of approximately 25% of power [29]. These calculations were carried out for average power values, not taking into account the number and type of electricity loads connected to the grid. A creep test machine consists of two systems: a heating system and a system responsible for generating a constant force. Thus, a typical creep test machine consists of a furnace in which the test specimen is placed, a lever system to which the test specimen is attached at one end, and a scale with weights at the other end [30,31]. The cited standard ISO 204:2023 requires that the temperature along the length of the test specimen and during the test is constant. The permissible temperature deviation is ± 3 °C for test temperatures below 600 °C. Due to such strict requirements, the furnaces of single-sample creep test machines are built as a three-zone system, using three electric heaters. Considering the number of machines used, the dimensions of the furnaces are limited, which consequently limits the space for the heaters. The placement of the resistance heaters in a small space, with the requirement to operate at high temperatures for long periods of time while being powered by 230 V mains voltage, results in their power rating being significantly higher than the typical power needed for the test. In the case under consideration, the power of the single furnace heater of the three-zone creep test machine is 1400 W, while the power of the lower heater, at a test temperature of 900 °C, does not exceed 400 W. The multi-sample machines are equipped with sixteen heaters for each heating chamber. There are 389 heaters connected to the electrical grid in the laboratory, respectively: 143 for phase L1, 130 for phase L2, and 116 for phase L3. Switching on all the heaters simultaneously would require a power source of 545 kW.

2.2. Heater Control

The instantaneous power characteristic for the power supply of the laboratory depends on the type of temperature controller used in the machines and, more specifically, on the type of actuator used. For continuous output controllers, where the power of the heater is changed by varying the voltage applied to the heater, the power characteristic of the laboratory is close to the average power and varies only slightly as a result of the controllers' response to disturbances affecting the object [32]. The use of continuous output controllers requires relatively expensive power amplifiers as actuators. The systems are also quite unreliable due to their complexity. In practice, in industrial systems, controllers with relay outputs are most commonly used for temperature control and SSR relays are used as the actuator [33]. This solution was implemented in the Creep Test Laboratory. The 389 independent relay controllers with inertia [34] were used to implement temperature stabilisation in the furnaces of the creep test machines. At the output of these controllers, a two-state signal is provided. Since the controllers are realised as discrete and operate with a sampling period of 200 ms, many times shorter than the values of the dominant time constants of the furnaces of the creep test machines, they are seen by the system as continuous PID controllers after filtering through the furnace. The use of this type of controller, instead of a classical PID controller, was motivated by economic reasons.

The creep test is supervised by an automatic system, which, on the hardware side, was realised on the basis of SIEMENS S7-300 series programmable controllers. The standard PID controller block has many functions and thus occupies quite considerable controller resources [35]. Therefore, it was decided to choose a custom solution dedicated to the needs of the laboratory; thus, a smaller number of controllers with fewer resources could be used. Figure 2 shows a model of the two-position temperature controller used in the furnaces of the creep test machines.
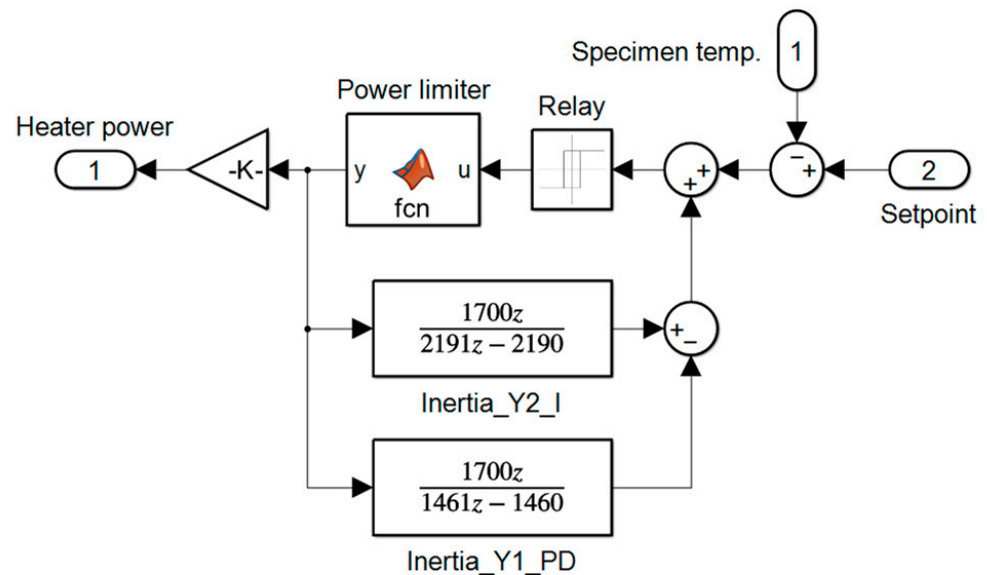

Figure 2. Model of a relay controller with inertia applied to temperature control in furnaces of creep test machines.

Placing in a single electrical network, 389 heaters of 1.4 kW independently controlled by relay could generate power peaks with an amplitude of up to several hundred kW. Therefore, several additional elements were used to reduce the occurrence of peaks in the considered system. Each of the temperature controllers used has a power limiter at its output, implemented in the form of a maximum heater-on time and by defining a minimum time between heater activations. A maximum heater-on time of 1.2 s and a minimum time between heater activations of 2.6 s were assumed. This corresponds to a signal filling of approximately 32%, which equates to a power output of 442 W. In addition, two independent synchronisation mechanisms were introduced to minimise power peaks: one for single-sample machines and one for multi-sample machines. The synchronisation mechanism for single-sample machines was constructed by placing the heaters in groups, where the master controller only allows one heater to be switched on at a time. For multi-sample machines, each chamber is considered an independent group. Only one heater can be switched on within a given chamber. This solution has reduced the occurrence of power peaks to around a maximum of 30 kW. Power variations at this level do not disrupt the mains grid. They also do not generate large disturbances in this grid. The problem occurs when the mains supply fails, and the laboratory switches to emergency power. In this case, a power source with a rated output of 75 kW is loaded with a continuous output of around 50 kW and peaks of 30 kW. The large power peaks on top of a relatively high average load value destabilise the speed controller of the diesel engine driving the alternator of the generator unit, resulting in the failure to stabilise the basic parameters, i.e., voltage and frequency, and consequently in an emergency shutdown of its. This is an unacceptable situation, as in the absence of power supply to the heaters, and consequently the inability to stabilise the temperature at a set level, an emergency shutdown of all ongoing tests is required.

2.3. The Problem of Reducing Power Peaks

There are at least several solutions to the presented problem, which can be divided into hardware and software solutions. By hardware solutions, we mean all those activities that require modifications to the existing infrastructure. Software solutions will be based solely on software modifications in PLC controllers installed in the laboratory. Mixed solutions can also be used. One example is the replacement of relay output controllers with continuous output controllers, where interference with the software of the programmable controllers is required, as well as the replacement of hardware components: cards with digital outputs by cards with analogue outputs and SSR electronic relays by analogue signal power amplifiers.

The hardware solutions for reducing power peaks also include reducing the power rating of the heaters. Due to the limitations of the furnace design, this cannot be completed by increasing the resistance of the heaters. Instead, the voltage supplied to the heater can be reduced, which simultaneously involves a power reduction. Reducing twice the voltage of a heater will result in a fourfold reduction in its power. This solution requires the use of transformers, which would incur high costs, require a space to be arranged for their installation, as well as the switching off of the power supply and the interruption of ongoing tests. Another solution could be to replace the existing power generator with another one with a much higher nominal power. Apart from the economic aspect, it should be noted that diesel generators should not be operated at low loads in relation to their nominal power [36]. A solution to filter power peaks at the power source side is the use of local energy storage, e.g., in the form of capacitor banks [37,38]. This solution is commonly used, for example, in electronic equipment, where a small capacitor is placed near the power supply of a digital chip to provide a source of energy for the large current peaks occurring when the digital gate transistors switch. Not placing capacitors near the power supply connection to digital chips results in destabilisation of the source seen from the side of that chip manifested by large voltage fluctuations [39].

Due to the need not to interrupt ongoing tests and, prospectively, to be able to adapt the laboratory for efficient use of energy from photovoltaic panels, it was decided to conduct research on software solutions. As creep tests are conducted in the laboratory, it is not possible to research power peak limiting algorithms in this environment. Therefore, it was decided to conduct research in the MATLAB Simulink simulation environment using the developed model of the laboratory [40]. The Creep Test Laboratory model was built based on models of creep test machine furnaces and control systems. The creep test machine furnace's models were developed by identification. An active identification experiment was conducted to collect the required data, which were used to develop a linear model, then completed with a static non-linearity correction [41]. The laboratory model was extended with a data exchange mechanism between the functions operating as the master controller and the functions processing the outputs of the temperature controllers. These are the equivalent of data exchange between programmable controllers on a Profibus network.

2.4. The Proposed Algorithm

The software solution to the problem of the occurrence of large power peaks in the electrical grid caused by unsynchronised switching on of a large number of heaters requires the development of an algorithm that will enable their activation to be scheduled in such a way as not to disturb the temperature control process in the creep test machine furnaces. It was assumed that the implementation of delays sufficiently short in relation to the dynamics of the furnaces would not significantly affect the temperature stabilisation on them. Two temperature deviations from the set point are defined in the laboratory, which triggers alarm states. A temperature rise of 0.5 °C above the set point generates a warning in the system, while a temperature rise of 1.0 °C or more above the set point interrupts the ongoing creep test. Considering that temperature disturbances not suppressed by the control system are typically 0.2 °C, it was assumed that heater switch-on delays, resulting from the operation of the power peaks minimisation algorithm, should not cause

temperature changes greater than 0.3 °C. In order to determine the maximum delays that can be inserted into the temperature control system of the furnace, an experiment was carried out in which the furnace model of a single-sample creep test machine was excited with a rectangular signal with constant filling while increasing its period. As a result, it was determined experimentally that for a period equal to 35 s, the temperature did not exceed the assumed deviations. The result of the experiment is shown in Figure 3. The value obtained was corrected by the average time between heater activations, with a minimum permissible temperature setpoint of 400 °C, in order to determine the permissible heater activation delays. On this basis, it was determined that the controller signal could be delayed up to 20 s while maintaining the assumed temperature deviations from the set point. Taking into account that the dominant time constant for single-sample machines is about 7200 s and for multi-sample machines it is about sixteen times higher, and that of the two determined permissible delay times, the shorter one should be chosen for further discussion, the experiment was not conducted for multi-sample machines.
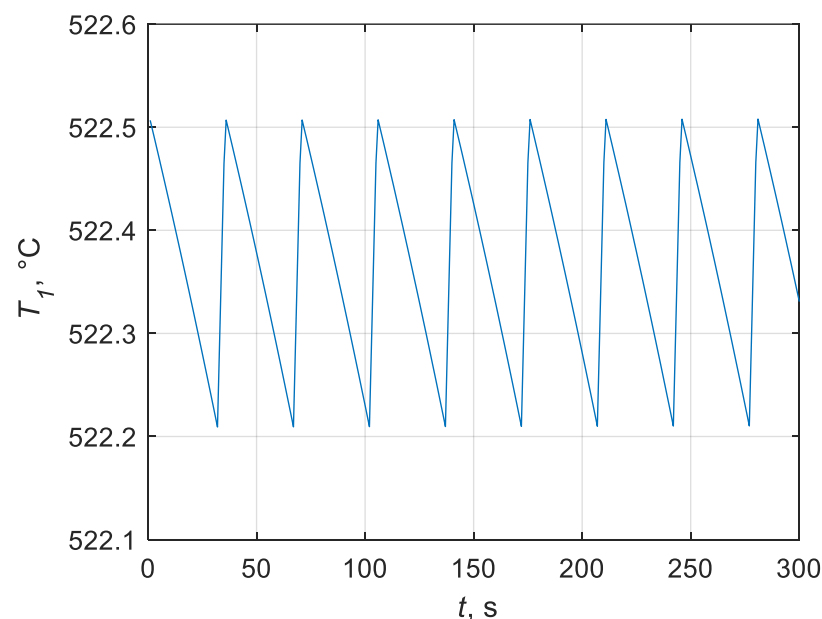

Figure 3. Temperature changes occurring in steady state, with an input signal of 10.1% duty cycle and a period of 35 s.

The developed algorithm for limiting power peaks occurring in the electrical grid uses a similar mechanism to a hardware solution based on a capacitor bank as a filter and energy storage at the same time [42]. Each temperature control system was extended with a software buffer placed between the controller output and the actuator. During the time the controller output is on, the buffer content is increased by one in the following sampling periods. During the time the heater is activated, the buffer content is decreased by one in the following sampling periods. The master algorithm decides when to turn on the heater. If the average buffer fill remains constant over the experimentally determined period, it can be expected that no exceedances of the permissible temperature deviations from the setpoint will occur. The task of the master algorithm is to determine the number of heaters to be switched on and then to select them. If the total power of the activated heaters is close to the average value determined in a certain time window, it should be expected that peaks will occur at most at the power level of a single heater. This effect is caused by quantised power values generated in the system as a result of relay control. The flow of the power through the buffers is shown in Figure 4.
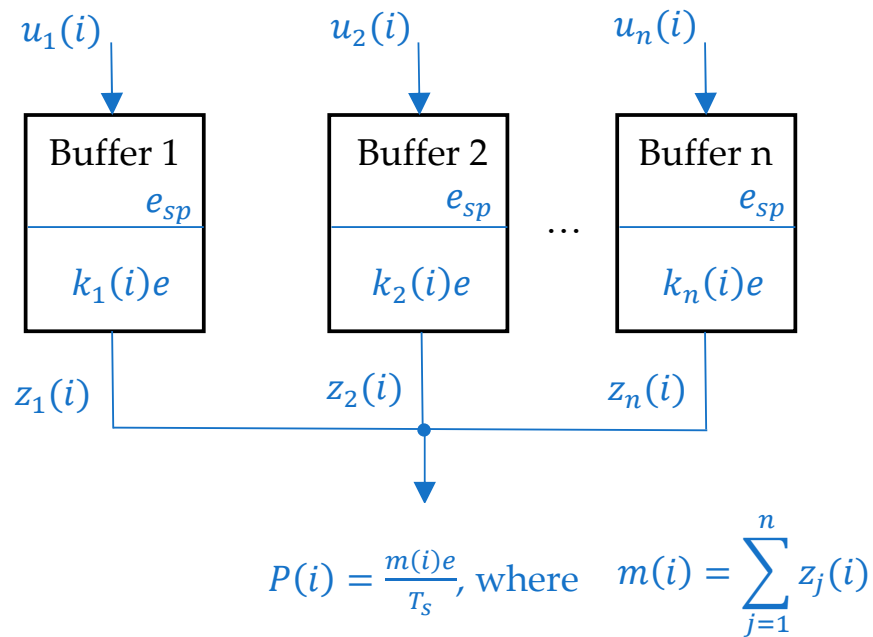
Figure 4. The flow of the power through the buffers.

The following notation is used here:

T_s—a sampling period of 200 ms used in the system under test;

$t_i = iT_s$—the i-th discrete time instant;

n—number of heaters;

$u_j(i) \in \{0,1\}$—the output of the controller of the heater j at a discrete time instant t_i;

$z_j(i) \in \{0,1\}$—state of the relay activating heater j at a discrete time instant t_i;

e—quantum of energy consumed by the switched on heater during the sampling period;

e_{sp}—buffered energy level set-point expressed as the number of quanta e;

$k_j(i)$—number of units in the heater buffer j at discrete time instant t_i;

$m(i)$—number of heaters switched on at a discrete time instant t_i;

$P(i)$—power source load at a discrete time instant t_i.

The equation for k_j at time t_i is as follows:

$$k_j(i) = k_j(i-1) + u_j(i) - z_j(i-1). \tag{1}$$

In each time sample, the number l of buffers in which the level of stored energy is greater than the assumed set level e_{sp} is determined. The number of heaters that should be switched on indicates the level to which the system should move in a smooth way. By operating on the number of machines being switched on instead of controlling them separately, this difficult multidimensional problem is reduced to a one-dimensional system, where the number of heaters to be switched on is determined by averaging the number of heaters waiting to be switched on. Therefore, a simple Proportional–Integral (PI) controller has been used, in which the input is a one-step prediction error of the number of machines to be switched on, and the output is the number of machines that will be switched on at a given time t_i. The applied controller with an integral element smoothly follows the changes by averaging the error signal e_r, thus not causing peak loads on the power source. The PI controller equation is described by the following formula:

$$m(i) = K\left(e_r(i) + \frac{T_s}{T_i}\sum_{k=0}^{i} e_r(i)\right), \tag{2}$$

where

$e_r(i) = l(i) - m(i-1)$ is a one step ahead prediction error;
$l(i)$—the number of buffers for which the level of stored energy is greater than e_{sp};
K—controller gain;
T_i—integration time.

The presented controller can be interpreted as a low-pass filter of changes in the input signal [43], which is the number of switched-on machines, causing a constant component to appear at its output corresponding to the value of the average power used to heat the machines. This component follows the average load of the electrical network as it changes due to the disturbances affecting the system under study. The PI controller used in the system operates as a low-pass filter for the power signal that should be used to maintain the filling of the virtual energy buffers at a constant level. These buffers are connected between the output of each of the furnace temperature controllers and the input of the actuator. The filling of these is related to the amount of energy going into them from the controllers and its release in the form of heater activation. Filling the virtual buffers at a constant level means that energy is continuously transferred from the regulators to the heaters. Maintaining the average filling of the buffers at a constant level allows the heater activations to be shifted in time. In order to achieve temperature stabilisation at a set level, the dynamics of the filter built on the PI controller should be chosen to match the dynamics of the object, which is the furnace of the creep test machine.

The developed algorithm specifies the number of heaters to be switched on at time t_i but does not specify exactly which heaters should be switched on. Considering that the number of heaters to be switched on is not the same as the number of buffers where the set level e_{sp} has been exceeded, they cannot be selected in a random manner. It is logical to first switch on those heaters for which the buffer is most full. However, adopting such a selection criterion may result in the fact that heaters for which the controllers rarely switch on the output will never heat. Therefore, the criterion for selecting a heater to switch on was completed by examining the time elapsed since it was last switched on. This criterion is the product of the buffer fill and the period of time that has elapsed since the related heater was switched on:

$$Q = \begin{bmatrix} k_1(i) * t_{off1}(i) \\ k_2(i) * t_{off2}(i) \\ \vdots \\ k_n(i) * t_{offn}(i) \end{bmatrix} \tag{3}$$

where:

Q—a vector of coefficients based on which the heaters are selected for activation (priority is given to the heaters with the highest coefficient values);
$t_{offj}(i)$—discrete time elapsed since the heater was last switched on.

The selection of the individual heaters to be switched on at time t_i is then achieved by picking $m(i)$ successive maximum values from the vector Q according to the iterative algorithm:

$$\forall g \in \{1, 2, \ldots, m\} : \exists j : \max(Q) > 0 \Rightarrow Q(j) = 0 \wedge H(j) = 1 \tag{4}$$

where:

m—number of machines to be switched on;
Q—a vector of coefficients based on which the heaters are selected for activation;
H—vector defining the state of the heaters: 1 for on, 0 for off.

By selecting the maximum values from the vector Q, the filling of the buffers is optimised [44] so that their value oscillates within a small range around the set value of their filling, resulting in the minimum values of the power peaks occurring in the electrical network. The flowchart of the algorithm is shown in Figure 5.
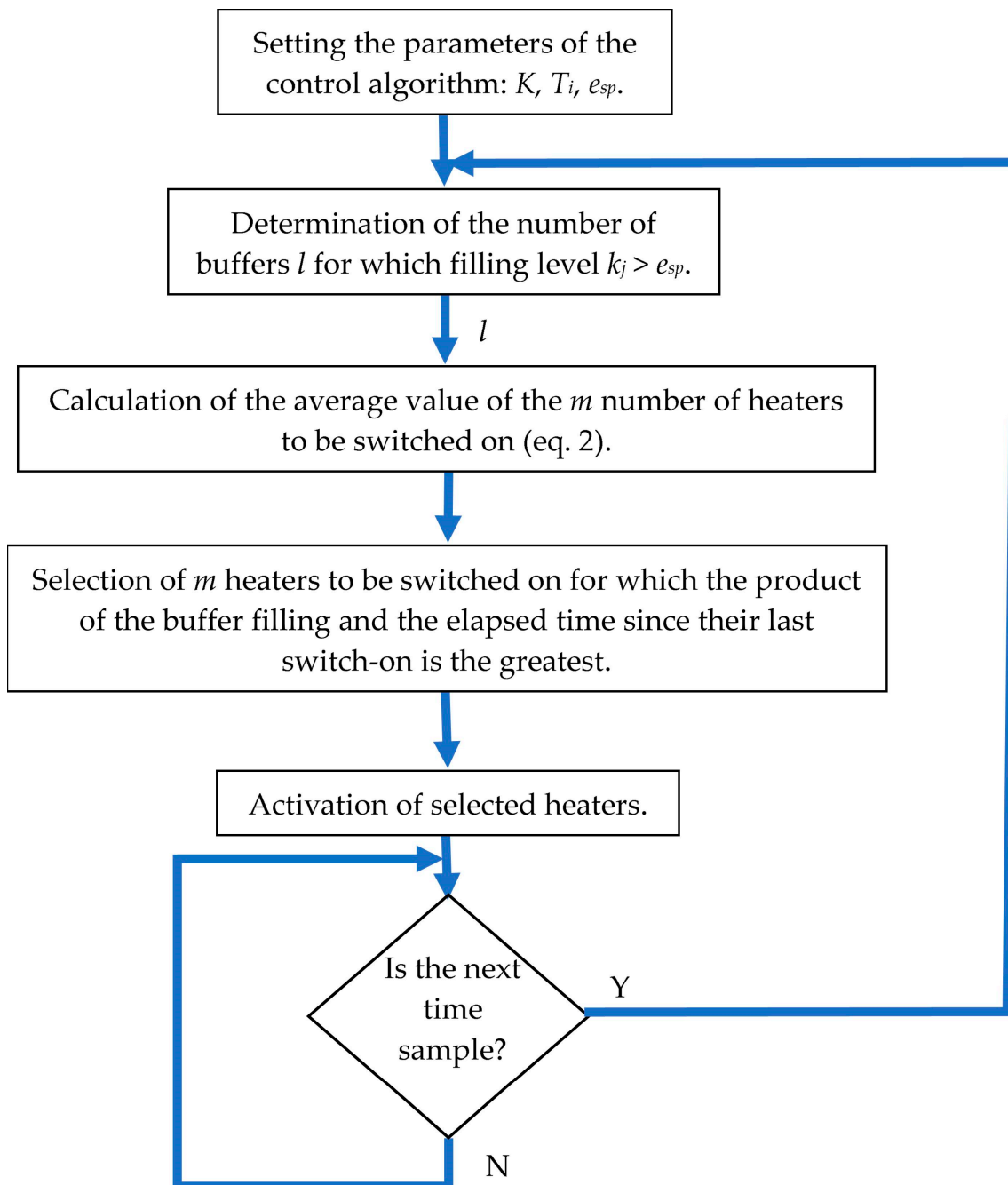
Figure 5. Flowchart of the applied methodology.

3. Results

The proposed method was tested by simulation to assess the impact of the algorithm parameter selection on its efficiency. Additionally, at first, it was checked how the system behaves without load synchronisation. Testing was divided into several steps. In each of them, the effect of changes in one parameter of the algorithm on the level of limiting power peaks and temperature variation in the furnaces of the creep test machines was studied. A flowchart of the research carried out is shown in Figure 6.
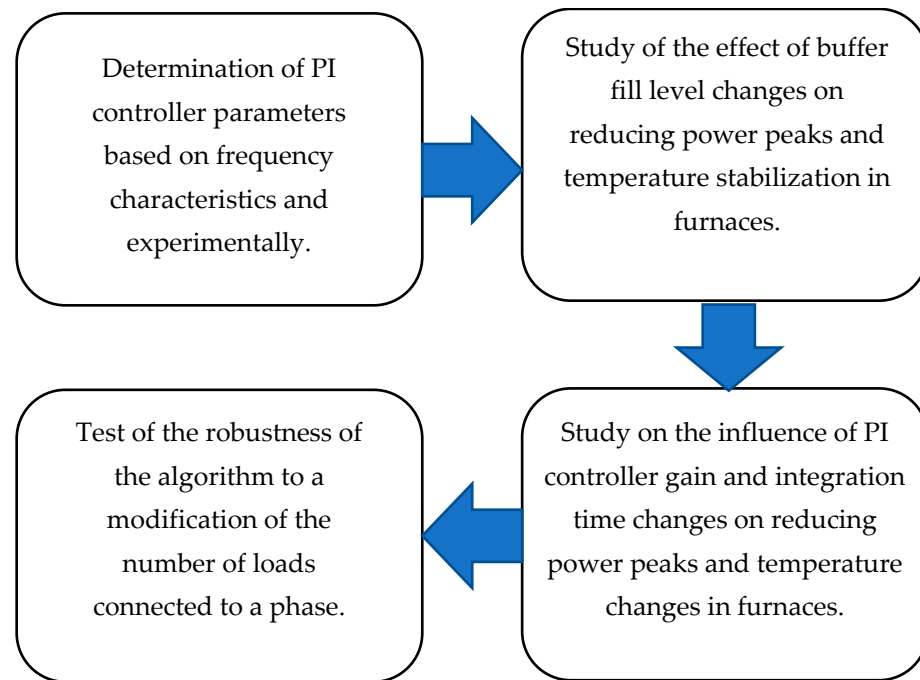
Figure 6. Flowchart of the conducted research.

3.1. Results Without Synchronisation

A simulation test was performed to examine the power waveform when the heaters were activated without synchronisation. Unsynchronised switching of 389 heaters with a power output of 1.4 kW each can generate a power peak of up to 545 kW. However, due to the disturbances affecting the object, switching of the heaters is distributed in time, so the total power of the system has a much smaller deviation from the average value. Nevertheless, it is still unacceptable. Figure 7 shows the simulated power trend in the absence of synchronisation between heater activations and the standard deviation σ, which is a measure of the occurring power disturbances. In all simulation tests presented below, the standard deviation was calculated for a time period of 50,000 s.
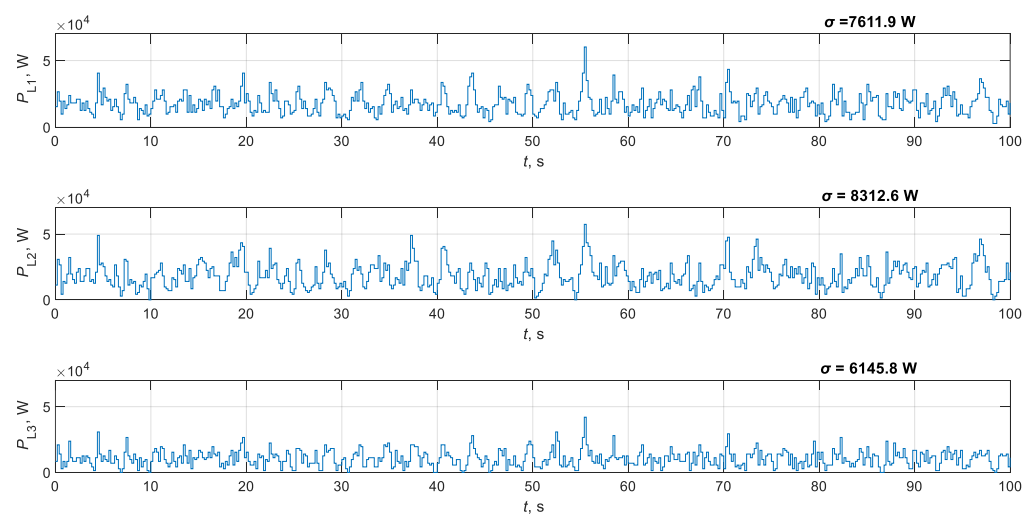
Figure 7. Simulated power waveform in the creep test laboratory without synchronisation between heater activations.

As a comparison, the real power peaks measured in the Creep Test Laboratory using a network quality meter Fluke 1738 are shown in Figure 8. The graph is shown as a waveform of minimum and maximum values measured within a one-second period. The power peaks in the real system are smaller. This is caused by appropriate software systems whose task is to reduce them. They also contain an additional DC component due to the load on the air conditioning system.
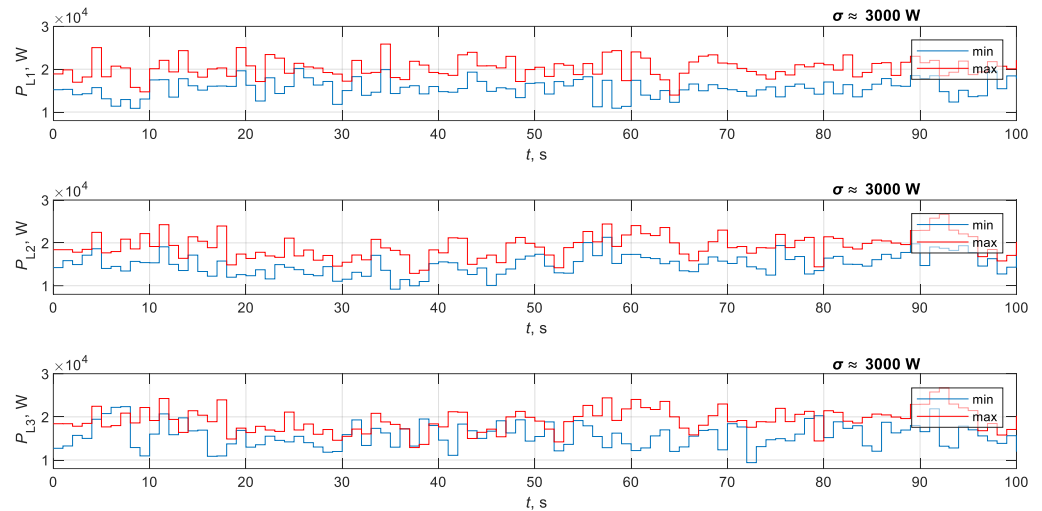

Figure 8. Maximum and minimum power values measured with a period of 1 s in the Creep Test Laboratory.

The temperature fluctuations occurring for a representative PJ17 creep test machine for the real (a) and simulated (b) systems are shown in Figure 9.
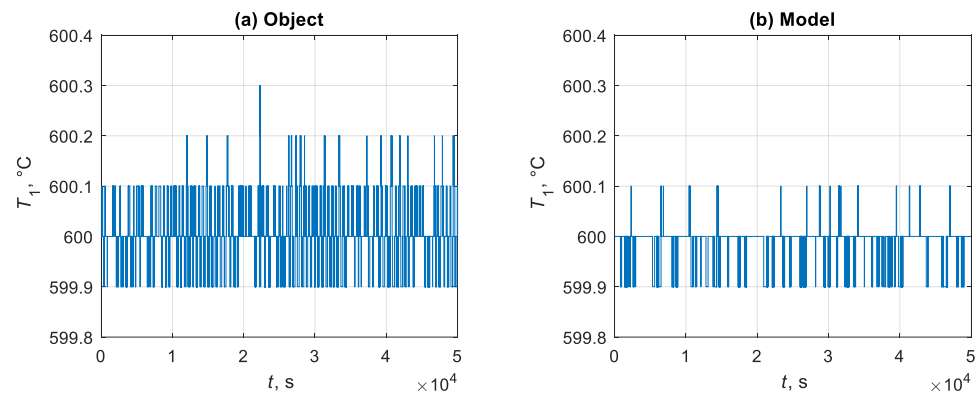

Figure 9. Temperature of zone 1 of the PJ17 furnace of a one-sample creep test machine (**a**) a real object, (**b**) a model simulated in the MATLAB Simulink environment.

3.2. Tuning the PI Algorithm

Due to the limitation of the long simulation time of the creep test laboratory model, the initial values of the PI controller parameters were found based on an analysis of the frequency characteristics of the created low-pass filter. The parameters were chosen in such a way that the dynamic of the filter was close to that of the linear part of the furnace model of the single-sample creep test machine. Then, the quality of the control and the conditions were checked for compliance with the permissible temperature deviations in the furnace in running simulations of the creep test laboratory model. For PI controller parameters of $K = 0.01$, $T_i = 50$ s, $e_{sp} = 50$, at steady state, with little disturbance, the system behaves stably, and power peaks are at the level of switching on one heater. The temperature in the

furnaces at steady state varied within 0.5 °C. However, for the heating state of the furnaces, or a large power fluctuation caused, for example, by several furnaces shutting down, the system became temporarily unstable. This is easily explained because the furnaces of the creep test machines are non-linear objects and, consequently, their characteristics differ significantly from those of the linear model whose characteristics were compared. Therefore, the parameters were experimentally changed by reducing the pass bandwidth of the filter. Testing in a simulation environment was carried out in order to determine experimentally the optimal parameters of the designed algorithm, as well as to determine the value of the margin around the optimal parameters, which does not cause a significant increase in power peaks. The frequency characteristics of the linear model of the creep test machine furnace and the low-pass filter are shown in Figure 10. The parameters of the control algorithm, which are the starting point for further research, are presented in Table 1.
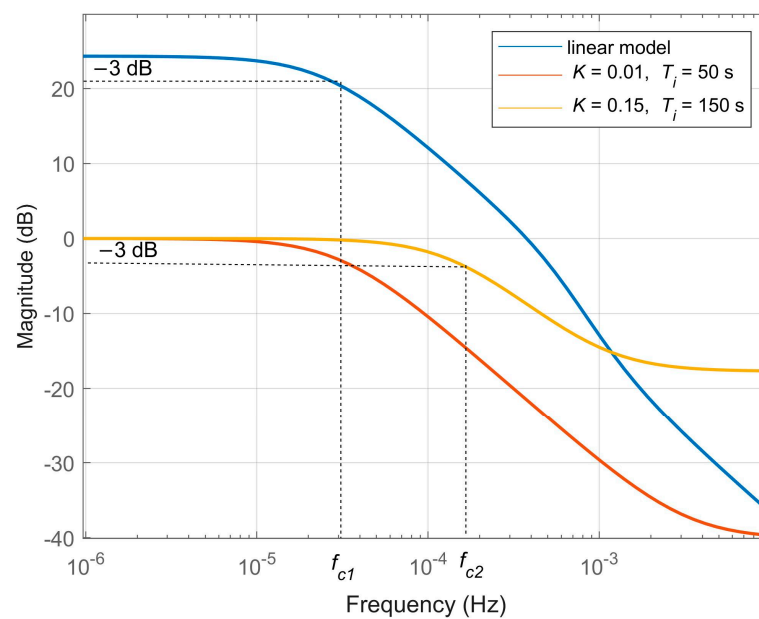

Figure 10. Frequency characteristics of the zone 1 furnace model of a single-sample creep test machine and the filter used in the power peaks limiting algorithm.

Table 1. Experimentally determined parameters of the algorithm limiting power peaks for the creep test laboratory model.

Parameter	Value
K	0.15
T_i	150
e_{sp}	50

Figure 11 shows the power waveforms for phases L1, L2, and L3 obtained for the laboratory model and the parameters presented in Table 1. Regarding the waveforms for non-synchronised control, a significant attenuation of the power peaks can be observed, which confirms the efficiency of the applied algorithm. Due to the asymmetry of the number of heaters connected to the particular phases, differences in damped peaks can be noticed between them, however, they are not significant. Therefore, in the following part of the article, due to the fact that the parameter changes give similar results for each phase, the results will be presented only for phase L1.
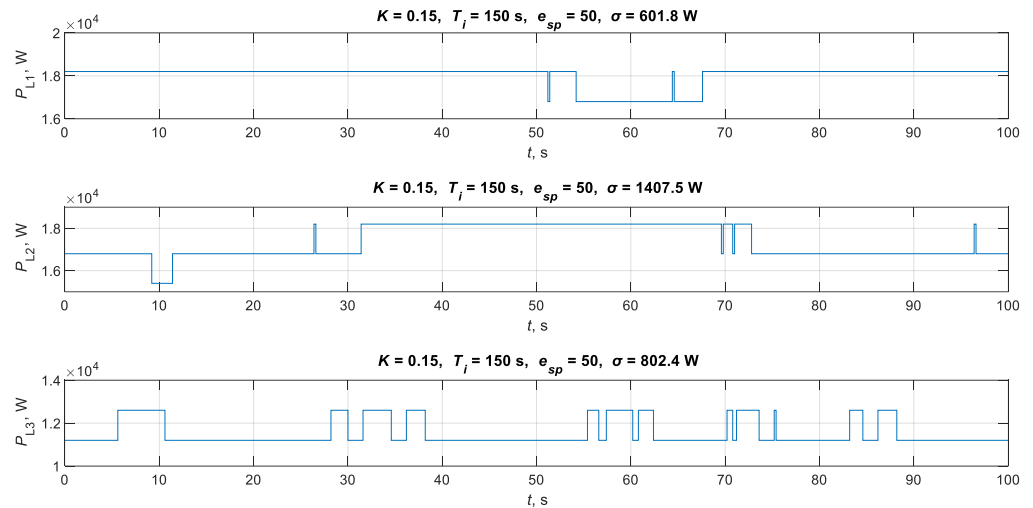
Figure 11. Simulated power waveform of the creep test laboratory after applying an algorithm to limit the power peaks using experimentally adjusted parameters.

3.3. Selecting the Buffer Fill Level

Taking into account that the idea of the algorithm was based on the application of buffers located between the output of the temperature controllers and the actuators, the effect of changes in the nominal value of the buffer filling on the shape of the laboratory's power characteristic was first investigated. Figure 12 shows the graph of power variation for a fixed buffer value e_{sp} of 1, 4, 50, and 200, and the determined standard deviation σ.
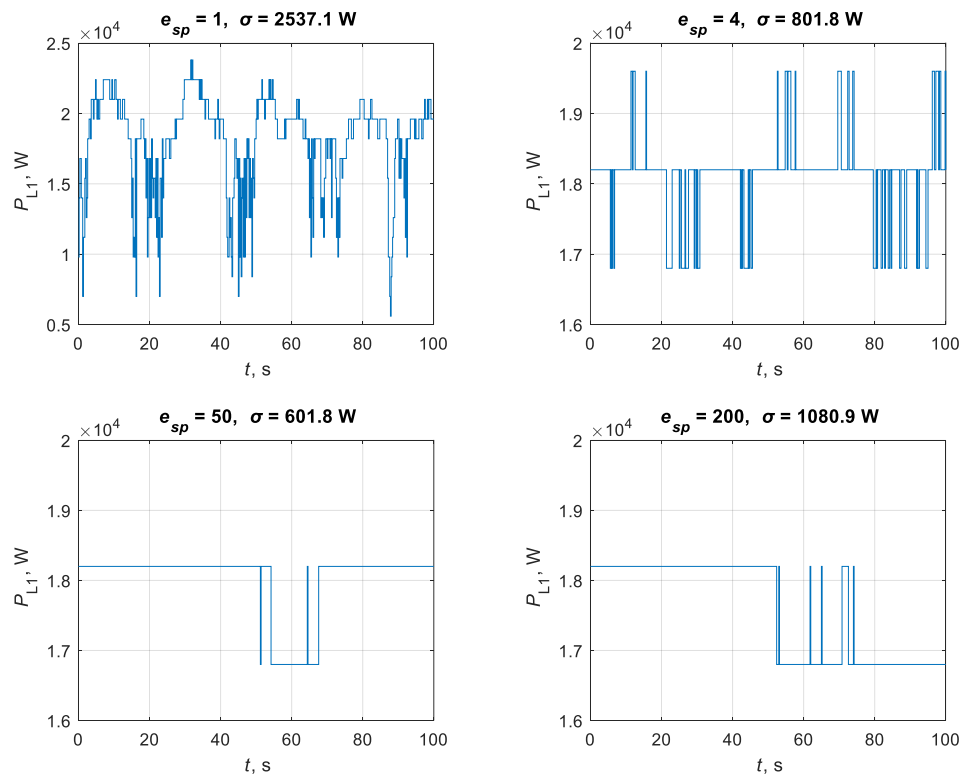

Figure 12. Simulated power waveform of phase L1 of the algorithm limiting power peaks, with different set values of the buffer fill level e_{sp}.

Figure 13 shows the temperature fluctuations occurring for a representative creep test machine for buffer fill values $e_{sp} = 50$ and $e_{sp} = 200$.
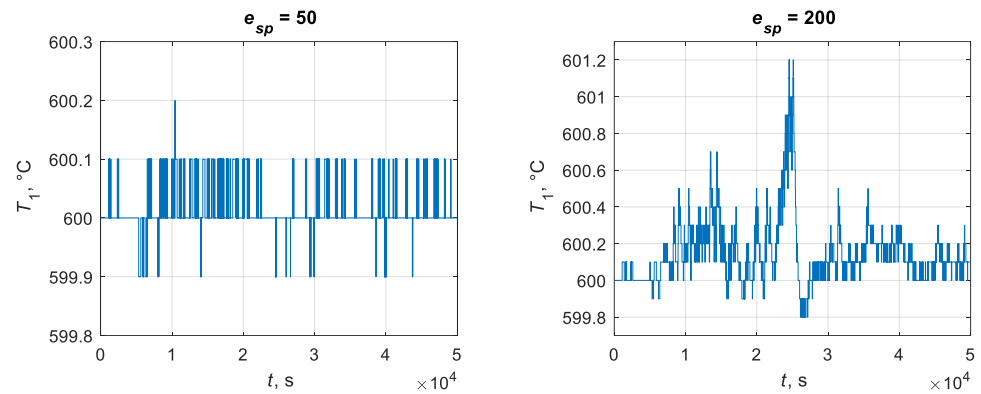
Figure 13. Temperature of zone 1 of the PJ17 furnace of a one-sample creep test machine at buffer e_{sp} fill levels of 50 and 200.

3.4. Testing the Impact of PI Controller Parameters

A similar investigation was carried out to observe the effect of different PI gain values on the characteristics of the power waveform and its variance. The test was carried out with the gain *K* varying from 0.0375 to 0.3. Figure 14 shows the power variation of the tested system for four representative values of *K*.
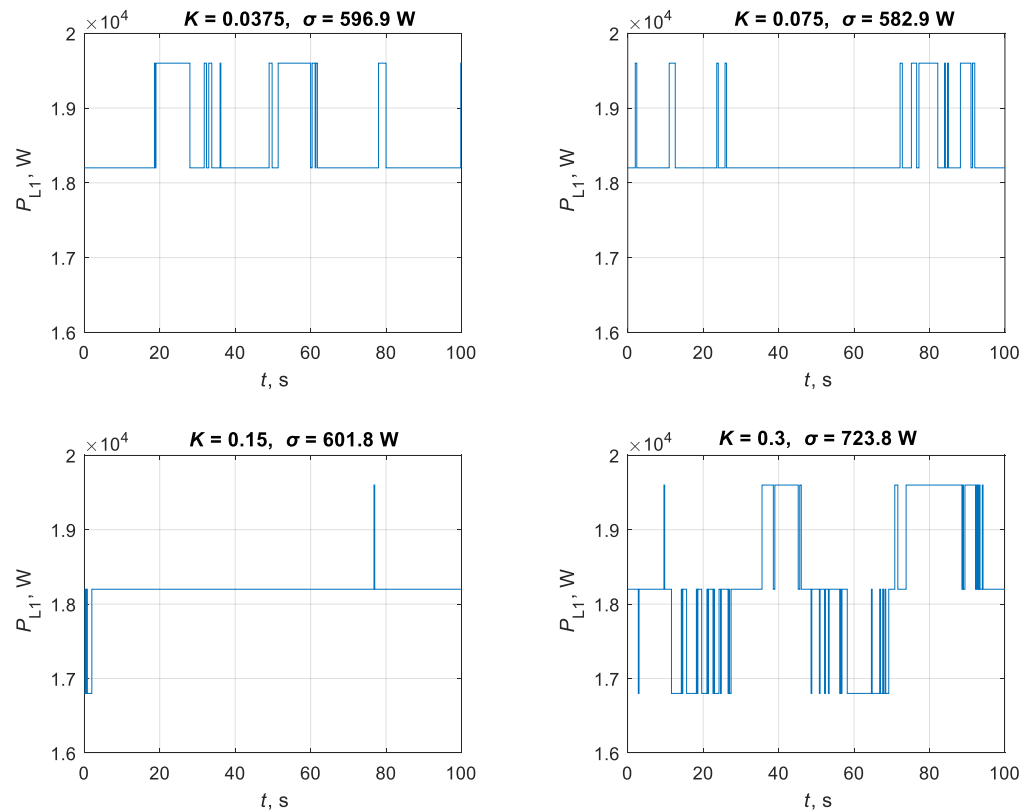

Figure 14. Simulated power waveform of phase L1 of the algorithm limiting power peaks, with various gain values *K* in the PI controller.

Figure 15 shows the temperature fluctuations occurring for a representative creep test machine for two extreme values of gain *K* of the PI controller.
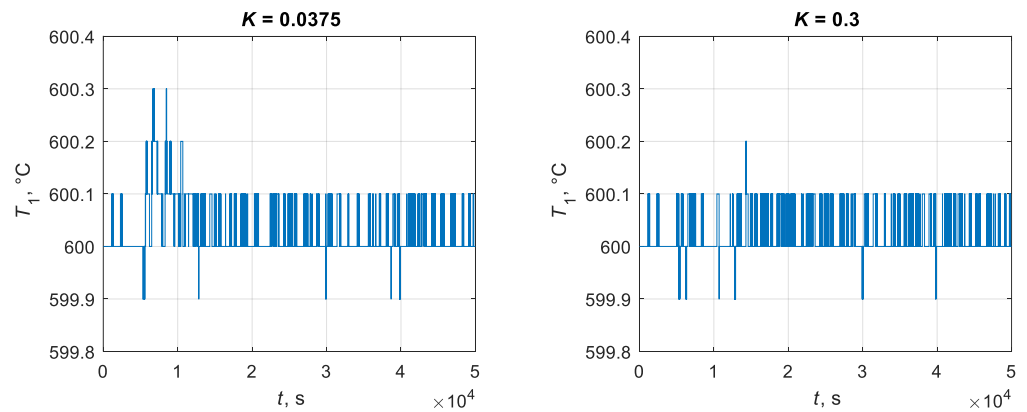
Figure 15. Temperature of zone 1 of the PJ17 furnace of a one-sample creep test machine at PI controller gain *K* values of 0.0375 and 0.3.

The effect of varying the integral time constant T_i for the PI controller on the characteristic changes in system power was also investigated. The test was carried out for varying the integration constant T_i in the range from 10 s to 800 s. The results of the test are shown in Figure 16.
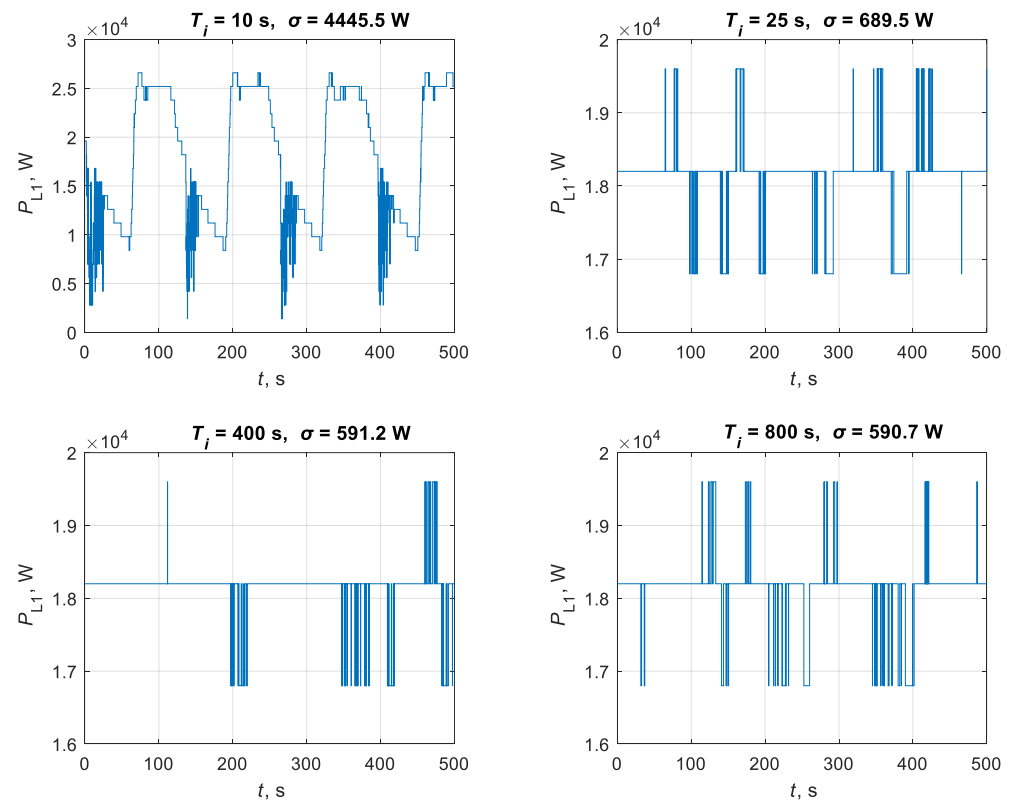

Figure 16. Simulated power waveform of phase L1 of the algorithm limiting power peaks, with different values of the integral time constant T_i in the applied PI controller.

Figure 17 shows the occurring temperature fluctuations for a representative creep test machine for two extreme values of the integral time constant T_i.
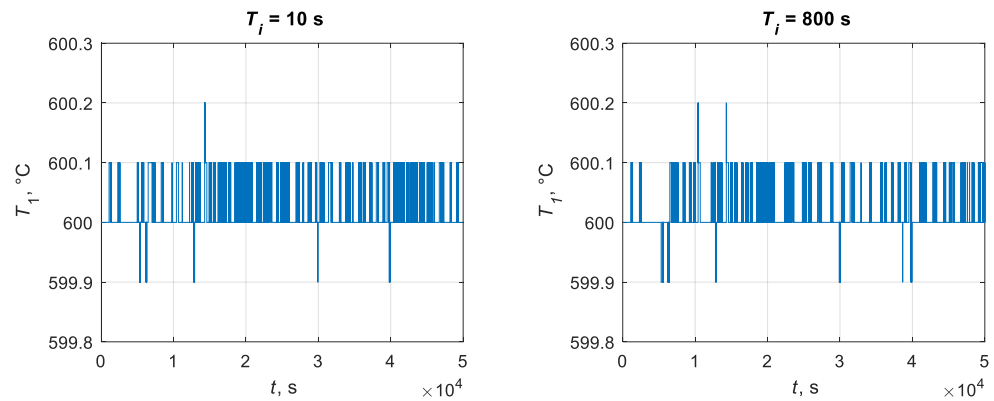
Figure 17. Temperature of zone 1 of the PJ17 furnace of a one-sample creep test machine at values of the integral time constant T_i of the PI controller equal to 10 s and 800 s.

3.5. Phase Load Differences

The tested system differs in the number of heaters connected to each phase, 143 heaters were connected to phase L1, 130 heaters to phase L2 and 116 heaters to phase L3. This means that 23% more heaters were connected to phase L1 than to phase L3. Due to the occurrence of asymmetry in the number of loads connected to the phases, it was checked whether the power waveforms would have a similar shape for the same parameters. Differences in the time characteristics of the power for particular phases were observed for large values of the buffer fill level e_{sp}. The power versus time graphs for the three phases for $e_{sp} = 100$ are shown in Figure 18. The graph shows that for phase L2, the power peaks are much higher than for the others, which suggests that in this case, the parameter e_{sp} can be better selected.
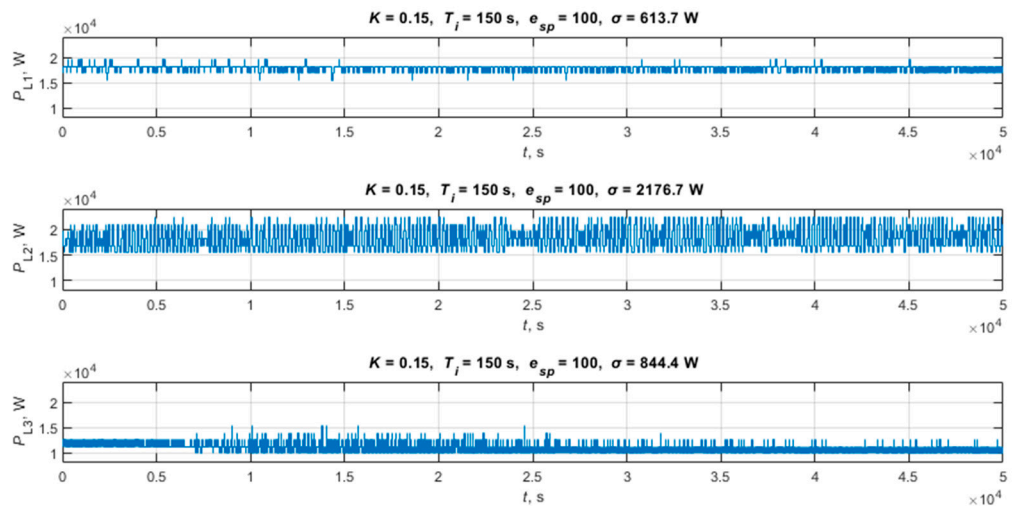

Figure 18. Simulated power waveform for the applied algorithm limiting power peaks at equal parameters for all phases.

Through the selection of the e_{sp} parameter individually for each phase, the value of phase L2 was sought to obtain the minimum value of power peaks. Figure 19 shows the power characteristics where the e_{sp} parameter was selected as 50 for the L1 and L3 phases, while for the phase L2, it was 8.
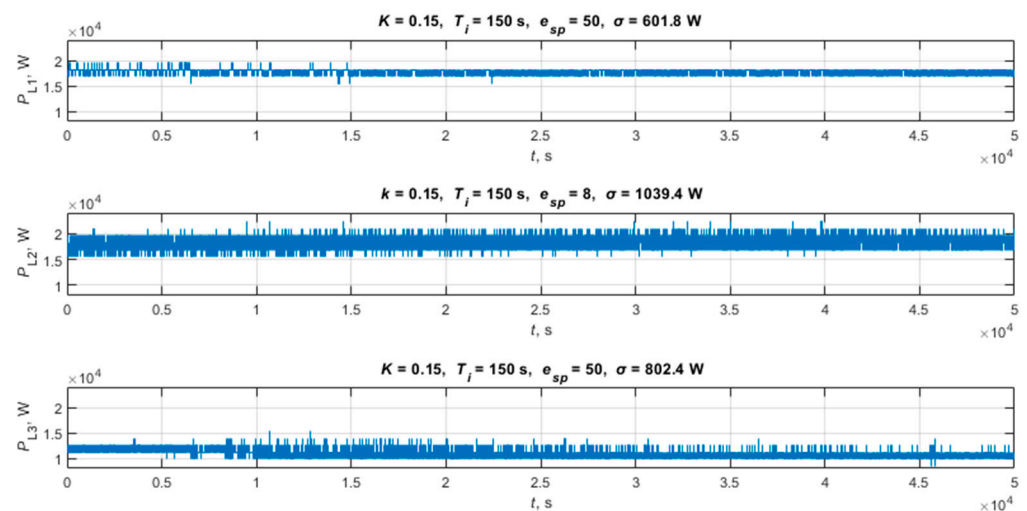
Figure 19. Simulated power waveform for the applied algorithm limiting power peaks with individual selection of parameter e_{sp} for each phase.

3.6. Discussion

The study confirmed the effectiveness of the developed algorithm in suppressing interference caused by asynchronous switching of electric heaters maintaining temperature in creep test machines. In the applied solution, buffering of temperature controller outputs has a significant impact on reducing power peaks occurring in the laboratory. In the absence of buffering (the value of e_{sp} is 1), power peaks reached 20 kW, while the standard deviation was 2.5 kW. Implementing the buffering of energy quanta at a relatively small level of $e_{sp} = 4$ reduces the standard deviation by almost four times, and the power peaks to about 4.2 kW. Raising the buffer level e_{sp} to 50 improves the characteristic in order to achieve power peaks corresponding to one or two heater activations, i.e., 1.4 or 2.8 kW. Also, small average power changes can be observed on the characteristic in the form of frequency modulation of the rectangular power signal with an amplitude of 1.4 kW, which corresponds to the rated power of a single heater. Increasing the buffer fill level above 100 degrades the power time waveform, and at an e_{sp} value of 200, the peak power reaches up to 16 kW. A large value of the average buffer fill level results in excessive power averaging, reducing the system's ability to follow the changes in the average power value. This condition also has a negative effect on the temperature stabilisation in the furnaces of the creep test machines, as illustrated in Figure 13. On the basis of the tests carried out, the level $e_{sp} = 50$ was determined, for which the quality of the power characteristics is best and for which the best standard deviation of 0.6 kW was achieved. It was also observed that changes in the buffer level value of the L1 phase between 15 and 85 do not significantly affect either the standard deviation of the system power or the stabilised temperature in the furnaces.

Changes to the PI controller parameters also have a fundamental impact on the shape of the power characteristic and the magnitude of the power peaks that occur. The PI controller, working as a low-pass filter, is responsible for following the changes in the average power value of the temperature controllers. Reducing the bandwidth too much causes the system not to follow the changes in the average power, resulting in too fast an emptying of the buffers and the occurrence of momentary oscillations of significant amplitude when the average power changes too much. This phenomenon was observed for very large values of the integral time constant T_i exceeding 800 s. On the other hand, small values of T_i resulted in oscillations in the power characteristics, e.g., for a T_i of 10 s, the peak-to-peak value of the oscillation was approximately 20 kW. These oscillations were caused by the PI controller having too wide a bandwidth, which resulted in insufficiently damped power peaks at its output caused by switching the heaters. The acceptable range of the integral time constant T_i not resulting in power peaks being transferred to the system output was from 50 s to 400 s. A value of $T_i = 150$ s was taken as the most suitable.

The gain K of the PI controller also affects the characteristics of the low-pass filter. Large gain values result in a direct transfer to the output occurring in the system power peaks. In the analysed system, these changes were observed for K equal to 0.3. At low values of gain K, the changes occurred at the level of one heater switch-on, while the system was exposed to the possibility of occurrence of momentary destabilisations manifested by the occurrence of single power peaks at the level of several kW. For the system under consideration, the value of gain K for which single power peaks were observed was 0.0375. The observed optimum value of gain K of the PI controller was 0.15, but its changes in the range of 0.075 to 0.2 had no significant effect on the observed power waveform. The low value of gain K caused larger temperature fluctuations in the creep test machine furnaces.

A discussion on the impact of changing the parameters of the peak-limiting algorithm was conducted using a single-phase example. The considered object for which the research was carried out uses a three-phase network, with single-phase electric heaters distributed between three phases. A different number of heaters were connected to each phase. In the conducted investigation, the power characteristics for each phase were compared, assuming that the algorithm parameters for all phases were the same. It was observed the influence of the buffer fill level value on the value of power peaks depending on the number of connected heaters. For a buffer fill level value of $e_{sp} = 100$, the smallest power peaks were observed in phase L1, to which the largest number of the heaters was connected. The other phases were characterised by a much greater destabilisation of the power time characteristics. This was also confirmed by the much larger standard deviation value determined for phases L2 and L3. Additionally, the occurrence of oscillations with a rather significant amplitude could be observed in phase L2. Depending on the number of heaters connected to the phase, the operating point shifts and the range of stable operation of the system narrows. By shifting the filling value of buffer e_{sp} from a value of 100 to a value of 8, the system was stabilised, and the power peaks for phase L2 were reduced. The optimum e_{sp} parameter value of 8 obtained for phase L2 is significantly lower than the optimum e_{sp} value of 50 specified for phases L1 and L3.

4. Conclusions

The aim of the study was to verify in a simulation environment an algorithm for limiting power peaks in an electrical grid in a multiple consumer two-position controlled system. The study was carried out on a model of an existing Creep Test Laboratory, where power peaks are caused by unsynchronised switching of 389 electric heaters. The presented algorithm was tested in a multi-load system characterised by high thermal inertia, including two types of energy consumers: furnaces of three-zone single-sample creep test machines and two-chamber furnaces of multi-sample machines, whose dominant time constant was about ten times greater. The parameters of the algorithm were adjusted to a smaller time constant, assuming that the delays caused by the algorithm would not affect the loads with a large time constant. This solution simplifies the master control system without using the much higher energy storage potential of high inertia loads, and it was possible to achieve a sufficient level of power peak suppression. As the algorithm does not distinguish between types of energy storage, it can be applied to grids with connected loads characterised by high thermal, electrical or mechanical inertia. The only condition is to ensure that the parameters of the algorithm are adjusted so that the switch-on delays for the loads with the shortest time constant do not cause the permissible deviations of the process variable to be exceeded.

Another issue is the limitation of power peaks in systems containing both loads with high inertia for the process variable and those with no or minimal energy storage capacity. In this case, the reduction of power peaks will be limited to energy storage loads only. This disadvantage for grids with mixed load types can be eliminated by developing and adding an additional module that, based on knowledge of the switching on of non-inertial devices, e.g., using predictive algorithms, will compensate the power peaks using the energy storage created from loads with high inertia.

The research demonstrated the effectiveness of the developed algorithm in systems where the controlled objects are characterised by relatively large time constants compared to the sampling period of the binary control signal. The authors also conducted research on reducing power peaks using task scheduling techniques. The problem of limiting power peaks was reduced to a task scheduling problem with a variable number of machines, and then, using heuristics, it was simplified. In this case, the obtained standard deviations were of the order of 0.5 kW, so similar or even slightly better than those presented in this article, but temperature stabilisation of the furnaces was not achieved. The slightly better suppression of power peaks was occupied by temperature changes in the furnaces of up to several degrees Celsius. In addition, the computational complexity of the task scheduling algorithm was significantly higher. The algorithm presented in this paper contained 20 lines of code in MATLAB. In comparison, the code of the task scheduling algorithm, after introducing the simplification, contained almost 400 lines of code. Thus, it can be concluded that for a system where the power does not change rapidly, the proposed algorithm based on power averaging represents a compromise between suppressing power peaks and not affecting the process variables of the connected loads. Because of its low computational complexity, it can be implemented in large industrial installations as well as installations using programmable controllers with low processor power.

The simplicity of the algorithm is due to its specific application in systems where the average power generated by the load changes slowly, as is the case in this particular installation. Obviously, this limits the application of the solution to a specific group of systems, where control is reduced to the stabilisation of a process variable. However, the idea itself is the beginning of a discussion on optimising the power of loads to gain benefits by increased self-consumption from local renewable sources or by enabling off-grid operation using the in-house power generator.

The resulting algorithm is a prelude to the development of algorithms that optimise power consumption according to its availability, with no impact or an acceptable impact on current process parameters. Implementing such algorithms in small installations is not a problem. Extending the problem to all devices connected to the electrical grid will require the implementation of specific communication standards as well as the expansion of various levels of control.

References

1. Antweiler, W. Cross-border trade in electricity. *J. Int. Econ.* **2016**, *101*, 42–51. [CrossRef]
2. Komorowska, A. Cross-border exchange of electricity between Poland and the neighbouring countries. *Polityka Energetyczna* **2019**, *22*, 37–52. [CrossRef]
3. Eghlimi, M.; Niknam, T.; Aghaei, J. Decision model for cross-border electricity trade considering renewable energy sources. *Energy Rep.* **2022**, *8*, 11715–11728. [CrossRef]
4. Thellufsen, J.Z.; Lund, H. Cross-border versus cross-sector interconnectivity in renewable energy systems. *Energy* **2017**, *124*, 492–501. [CrossRef]

5. Ueda, Y.; Kurokawa, K.; Tanabe, T.; Kitamura, K.; Sugihara, H. Analysis results of output power loss due to the grid voltage rise in grid-connected photovoltaic power generation systems. *IEEE Trans. Ind. Electron.* **2008**, *55*, 2744–2751. [CrossRef]
6. Collins, L.; Ward, J.K. Real and reactive power control of distributed PV inverters for overvoltage prevention and increased renewable generation hosting capacity. *Renew. Energy* **2015**, *81*, 464–471. [CrossRef]
7. Wang, L.; Yan, R.; Saha, T.K. Voltage regulation challenges with unbalanced PV integration in low voltage distribution systems and the corresponding solution. *Appl. Energy* **2019**, *256*, 113927. [CrossRef]
8. Rúa, J.; Verheyleweghen, A.; Jäschke, J.; Nord, L.O. Optimal scheduling of flexible thermal power plants with lifetime enhancement under uncertainty. *Appl. Therm. Eng.* **2021**, *191*, 116794. [CrossRef]
9. Viswanathan, R.; Stringer, J. Failure mechanisms of high temperature components in power plants. *J. Eng. Mater. Technol.* **2000**, *122*, 246–255. [CrossRef]
10. Barchi, G.; Miori, G.; Moser, D.; Papantoniou, S. A Small-Scale Prototype for the Optimization of PV Generation and Battery Storage through the Use of a Building Energy Management System. In Proceedings of the 2018 IEEE International Conference on Environment and Electrical Engineering and 2018 IEEE Industrial and Commercial Power Systems Europe, EEEIC/I and CPS Europe, Palermo, Italy, 12–15 June 2018.
11. Vieira, F.M.; Moura, P.S.; de Almeida, A.T. Energy storage system for self-consumption of photovoltaic energy in residential zero energy buildings. *Renew. Energy* **2017**, *103*, 308–320. [CrossRef]
12. Kousksou, T.; Bruel, P.; Jamil, A.; El Rhafiki, T.; Zeraouli, Y. Energy storage: Applications and challenges. *Sol. Energy Mater. Sol. Cells* **2014**, *120 Pt A*, 59–80. [CrossRef]
13. Olatomiwa, L.; Mekhilef, S.; Ismail, M.S.; Moghavvemi, M. Energy management strategies in hybrid renewable energy systems: A review. *Renew. Sustain. Energy Rev.* **2016**, *62*, 821–835. [CrossRef]
14. Almalaq, A.; Alshammarry, A.; Alanzi, B.; Alharbi, F.; Alshudukhi, M. Deep Learning Applied on Renewable Energy Forecasting Towards Supply-Demand Matching. In Proceedings of the 20th IEEE International Conference on Machine Learning and Applications, ICMLA, Pasadena, CA, USA, 13–16 December 2021; pp. 1345–1349.
15. Papkov, B.; Mahnitko, A.; Zicmane, I.; Berzina, K.; Lomane, T.; Veremiichuk, Y. System Approach to Management of Electrical Consumption in Intelligent Electrical Networks. In Proceedings of the 2019 IEEE International Conference on Environment and Electrical Engineering and 2019 IEEE Industrial and Commercial Power Systems Europe, EEEIC/I and CPS Europe, Genova, Italy, 11–14 June 2019.
16. Qureshi, J.A.; Gul, M.; Faruqi, M.A.; Qureshi, W.A. Intelligent demand management for end user benefits. In Proceedings of the 2011 IEEE PES Conference on Innovative Smart Grid Technologies—Middle East [ISGT Middle East 2011], Jeddah, Saudi Arabia, 17–20 December 2011.
17. De, A.S.M. Load shifting technique for reduction of peak generation capacity requirement in smart grid. In Proceedings of the 2016 IEEE 1st International Conference on Power Electronics, Intelligent Control and Energy Systems, Delhi, India, 4–6 July 2016.
18. Choi, H. Overview of charging technology evolution in smartphones. *J. Power Electron.* **2023**, *23*, 1931–1941. [CrossRef]
19. Reydarns, H.; Lauwereys, V.; Haeseldonckx, D.; Van Willigenburg, P.; Woudstra, J.; De Jonge, S. The development of a proof of concept for a smart DC/DC power plug based on USB power delivery. In Proceedings of the 22nd Conference on the Domestic Use of Energy (DUE 2014), Cape Town, South Africa, 1–2 April 2014; p. 6827761.
20. Marales, R.C.; Preda, S. Demand Side Managment Electric Energy Consumption Data Processing Architectures Within Internet of Things Context. In Proceedings of the IEEE Joint 19th International Symposium on Computational Intelligence and Informatics and 7th International Conference on Recent Achievements in Mechatronics, Automation, Computer Sciences and Robotics, CINTI-MACRo, Szeged, Hungary, 14–16 November 2019; pp. 43–48.
21. Laicane, I.; Blumberga, D.; Blumberga, A.; Rosa, M. Reducing household electricity consumption through demand side management: The role of home appliance scheduling and peak load reduction. *Energy Procedia* **2015**, *72*, 222–229. [CrossRef]
22. Moura, P.S.; López, G.L.; Moreno, J.I.; De Almeida, A.T. The role of Smart Grids to foster energy efficiency. *Energy Effic.* **2013**, *6*, 621–639. [CrossRef]
23. Mbungu, N.T. Control and estimation techniques applied to smart microgrids: A review. *Renew. Sustain. Energy Rev.* **2023**, *179*, 113251. [CrossRef]
24. Adam, Z. The role of Institute of Ferrous Metallurgy in the development of materials for the power industry. *J. Met. Mater.* **2021**, *73*, 3–8. [CrossRef]
25. Sroka, M.; Zieliński, A.; Golański, G.; Pawlyta, M.; Purzyńska, H.; Novy, F. Evolution of the microstructure and mechanical properties of Sanicro 25 austenitic stainless steel after long-term ageing. *Arch. Civ. Mech. Eng.* **2023**, *23*, 149. [CrossRef]
26. Purzyńska, H.; Golański, G. Incoloy 800HT iron-based superalloy-preliminary characterisation. *J. Met. Mater.* **2022**, *74*, 42–46. [CrossRef]
27. Altenbach, H.; Eisenträger, J. Introduction to Creep Mechanics. In *Encyclopedia of Continuum Mechanics*; Springer: Berlin/Heidelberg, Germany, 2019. [CrossRef]
28. *ISO 204:2023*; Metallic materials—Uniaxial Creep Testing in Tension—Method of Test. ISO: Geneva, Switzerland, 2023.
29. Iverson, J. *How to Size a Genset: Proper Generator Set Sizing Requires Analysis of Parameters and Loads*; Cummins Power, Technical Information: Fridley, MN, USA, 2007; PT-7007 (03/07).
30. Momoh, J.J.; Ajueyitsi, O.N.A.; Onipede, A.I.M. Development of a Low Cost Mechanically Operated Tensile and Creep Testing Machine. *J. Eng. Appl. Sci.* **2008**, *3*, 491–495.

31. Molina, R.; Pender, G.; González, G.; Moro, L. Checking of the uniformity of results of simultaneous creep testing equipment. *Rev. Mater.* **2018**, *23*, e-12022.

32. Rooholahi, B.; Reddy, P.L. Concept and application of PID control and implementation of continuous PID controller in Siemens PLCs. *Indian J. Sci. Technol.* **2015**, *8*, 9. [CrossRef]

33. Gurevich, V. *Electric Relays: Principles and Applications*; CRC Press: Boca Raton, FL, USA, 2018.

34. Hudy, W.; Jaracz, K.; Migo, P. Analysis of a two-position regulation system with correction. *Ann. Univ. Paedagog. Cracoviensis Stud. Tech.* **2017**, *10*, 30–34.

35. SIMATIC Standard PID Control Manual. edition 03/2003, SIEMENS. Available online: https://cache.industry.siemens.com/dl/files/084/1137084/att_27126/v1/Stdpid_e.pdf (accessed on 8 September 2024).

36. Mobarra, M.; Rezkallah, M.; Ilinca, A. Variable Speed Diesel Generators: Performance and Characteristic Comparison. *Energies* **2022**, *15*, 592. [CrossRef]

37. Hadjipaschalis, I.; Poullikkas, A.; Efthimiou, V. Overview of current and future energy storage technologies for electric power applications. *Renew. Sustain. Energy Rev.* **2009**, *13*, 1513–1522. [CrossRef]

38. Espinar, B.; Mayer, D. *The Role of Energy Storage for Mini-GRID Stabilization*; Report IEA-PVPS T11-02:2011, hal-00802927; International Energy Agency: Paris, France, 2011.

39. OTT, H.W.; OTT, H.W. *Noise Reduction Techniques in Electronic Systems*; Wiley: New York, NY, USA, 1988.

40. Chaturvedi, D.K. *Modeling and Simulation of Systems Using Matlab® and Simulink®*; CRC Press Taylor & Francis Group, LLC: Abingdon, UK, 2010.

41. Szulc, M.; Kasprzyk, J.; Loska, J. Creep Testing Machine Identification for Power System Load Optimization. *Lect. Notes Netw. Syst.* **2023**, *708*, 113–122.

42. Xue, S.; Che, Y.; He, W.; Zhao, Y.; Zhang, R. Control strategy of electric heating loads for reducing power shortage in power grid. *Processes* **2019**, *7*, 273. [CrossRef]

43. Lower, M.; Dobrowolski, P. Application of the Closed-Loop PI Controller as the Low-Pass Filter. In *Theory and Engineering of Dependable Computer Systems and Networks, Proceedings of the Sixteenth International Conference on Dependability of Computer Systems DepCoS-RELCOMEX, Wrocław, Poland, 28 June–2 July 2021*; DepCoS-RELCOMEX 2021, Advances in Intelligent Systems and Computing; Springer: Cham, Switzerland, 2021; Volume 1389, p. 1389. [CrossRef]

44. Koutsopoulos, I.; Tassiulas, L. Control and optimization meet the smart power grid: Scheduling of power demands for optimal energy management. In Proceedings of the 2nd International Conference on Energy-Efficient Computing and Networking, New York, NY, USA, 31 May–1 June 2011; ACM International Conference Proceeding Series 2012. pp. 41–50.